Materials Research. 2010; 13(1): 29-34

Microstructural and Nonohmic Properties of $ZnO.Pr_6O_{11}$ CoO Polycrystalline System

***Miguel Angel Ramírez*[a]*, *José Francisco Fernández*[b], *José de Frutos*[c], *Paulo Roberto Bueno*[a], *Elson Longo*[a], *José Arana Varela*[a]**

[a]*Instituto de Química, Universidade Estadual Paulista – UNESP, 14801-970 Araraquara - SP, Brazil*
[b]*Instituto de Cerámica y Vidrio, Departamento de Electrocerámica, 24049, Madrid, España*
[c]*ETSIT, Universidad Politécnica de Madrid, Ciudad Universitaria, 28040, Madrid, España*

Received: May 6, 2009; Revised: December 7, 2009

The microstructure and electrical properties of varistors composed of (95-x) ZnO + x Pr_6O_{11} + 5 CoO (ZPC), (x = 0.1, 0.5 and 1.0) and sintered at 1300 and 1350 °C, were investigated. According to X-ray diffraction, several phases (ZnO, Pr_2O_3 and Pr_2CoO_4) are present when x = 1.0. Using Scanning Electron Microscopy, all of these compositions contain precipitates. These phases are important regarding the development of the microstructure and the electrical properties. The samples with x = 0.1 introduce the best nonohmic behavior (α = 9.0), however when x = 0.5 the electrical properties are highly degraded due to the small quantity of effective barriers. The density of superficial states N_{IS} and donor concentration *Nd* decreases with Pr_6O_{11} addition. The decrease in the donor concentration is attributed to the annihilation of the donor defects according to the transformation of praseodymium oxides from Pr_6O_{11} to Pr_2O_3.

Keywords: *electrical properties, varistors, grain boundary, microstructure*

1. Introduction

ZnO varistor ceramics are resistor devices manufactured by sintering ZnO powder containing various minor additives[1]. It has been recognized that at least two different classes of additives must be added to the ceramic varistors in order to obtain good nonohmic characteristics[2]. The first class of such additives are varistor-forming oxides (VFO), such as Bi_2O_3, Pr_6O_{11}, La_2O_3, BaO, V_2O_5 and glass frits. The second class of additives are 3d transition-metal oxides, which improve significantly the nonohmic characteristics[3]. Zinc oxide ceramics, containing Pr_6O_{11} and CoO, which exhibit current nonohmic characteristics, were first reported by Mukae et al.[4]. In fact, the history of Pr_6O_{11}-based ZnO varistors is similar to the Bi_2O_3-based ZnO varistors[5], but they have not been adequately studied. However, the Pr_6O_{11}-based ZnO varistors don't have volatilization of components[3] and they own a simpler microstructure when compared with Bi_2O_3-based varistors, which is an important fact for the stability and degradation phenomena[6-9]. Most of commercial ZnO varistors are ZnO-Bi_2O_3-based varistor ceramics, possessing as major additive Bi_2O_3. Although they exhibit excellent varistor performance, they possess few drawbacks due to the high volatility and reactivity of Bi_2O_3 at a sintering temperature above 1000 °C[10]. Another flaw of Bi_2O_3-based varistors is that they need many additives to obtain high nonlinearity and stable electrical properties. ZnO varistors generally contain three phases, such as ZnO grains, Bi_2O_3-rich intergranular layer and spinel particles[10]. To overcome the problems in Bi_2O_3-based varistors, ZnO varistors using praseodymium oxides as VFO have been reported[3-5, 11-12]. On the other hand, Pr_6O_{11}-based ZnO varistors are reported to have only two-phases detected by X-ray diffraction, namely, ZnO grains and intergranular layers enriched with praseodymium[13]. The absence of a spinel phase increases the active grain boundary area through which the electrical current flows. Therefore, the effective cross-section area of the elements is increased[14]. Several studies describe the dependence of varistor properties on processing conditions of Pr-doped ZnO varistors, especially in the field of grain boundary formation[2-4, 13]. It is very important to understand the structure, composition and properties of the boundaries since they have a strong influence on electrical properties. Our purpose is to investigate the microstructure, the current density-electric field (*J* vs. *E*) characteristics, and the capacitance-voltage (*C-V*) characteristics of ZPC varistor systems.

2. Experimental Procedure

The varistor systems (95-x) mol% ZnO + x mol% Pr_6O_{11} + 5 mol% CoO (x = 0.1, 0.5 and 1.0) were prepared from the mixture of oxide precursors method, all of them being analytical grade oxides: ZnO (Aldrich-99.99%), Pr_6O_{11} (Aldrich-99.9%) and CoO (Riedel-99.9%). The starting materials were attrition-milled in water for 3 hours. Then the dry slurry was calcined at 750 °C in air for 2 hours. The calcined powders were pulverized using agate mortar and pestle and after 2 wt. (%) polyvinyl alcohol (PVA) binder addition, granulated by sieving 200-mesh screen to produce the starting powder. The powder was uniaxially pressed into discs of 12 mm diameter and 1 mm thickness at a pressure of 80 MPa. The pellets were sintered at 1300 and 1350 °C for 2 hours with a heating rate of 5 °C/min followed by furnace cooling. The samples were characterized by X-ray diffraction (XRD, Rigaku, 20-2000), 40 kV and 150 mA from 2θ (20 to 80°), $\Delta 2\theta = 0.02°$, with Cukα wavelength monocromatized by a graphite crystal. To obtain the Scanning Electron Microscopy (SEM) micrographies (ZEISS® DSM 940 A) the sintered samples were polished and thermally etched by heating at 100 °C below the

*e-mail: margbrasil@yahoo.com

sintering temperature during 30 minutes The average grain size (*d*) was determined by the linear intercept method, given by $d = 1.56\ L/MN$, where *L* is the random line length on the micrograph, *M* the magnification of the micrograph, and *N* is the number of the grain boundaries intercepted by lines[15]. Gold contacts were deposited on the samples surfaces by sputtering in order to measure the nonohmic properties. Current-voltage measurements were taken by using a High Voltage Measure Unit (Keithley Model 237). The breakdown electric field (*Eb*) was obtained at a current density from 1 mA.cm^{-2} and the leakage current I_L was measured at 0.80 *Eb*. In addition, the nonlinear coefficient (α) was determined from linear regression of *log J* vs. *log E* in the 1-10 mA.cm^{-2} region. The impedance measurements were made with a frequency response analyzer (HP 4294 A LF) using frequency ranging from 40 Hz up to 110 MHz. The capacitance-voltage (*C-V*) characteristics of ZPC varistors were measured as a function of frequency with the variable applied bias voltage (0-38 V). The donor concentration (*Nd*) of ZnO grains and the barrier height (ϕ_B) at the grain boundary were determined from the slope and intercept of straight line, respectively, using the Equation 1:

$$\left(\frac{1}{C}-\frac{1}{2C_0}\right)^2=\frac{2p^2}{qk\varepsilon_0 N_d}\left(\phi_B+\frac{V}{p}\right) \quad (1)$$

proposed by Mukae et al.[16]. In this equation *C* is the capacitance per unit area of grain boundary, C_0 is the capacitance when $V = 0$, *V* is the voltage applied per grain, *q* is the electronic charge, ε_0 is the permittivity of free space, *k* is the dielectric permittivity of ZnO (~8.5) and *p* is the number of barriers between grains (obtained by calculating the distance between electrodes divided by average grain size). The density of the interface states N_{IS} at the grain boundary was determined using the Equation 2:

$$N_{IS}=\left(\frac{2k\varepsilon_0 N_d\phi_B}{q}\right)^{\frac{1}{2}} \quad (2)$$

Once the donor concentration and barrier height are known, the depletion layer width (ω) of either side at the grain boundaries was determined by the Equation 3.

$$N_d\omega = N_{IS} \quad (3)$$

3. Result and Discussion

Figure 1a shows XRD pattern for the samples of the ZPC system sintered at 1300 °C. The samples with x = 0.1 and 0.5 contain only a wurtzite ZnO phase (card PDF 36-1451), while when x = 1.0, the sample contents a praseodymium sesquioxide phase, Pr_2O_3 (card PDF 47-1111), and exhibits a low intensity peak of Pr_2CoO_4 (card PDF 34-1282). XRD pattern for the samples sintered at 1350 °C are shown on Figure 1b. The difference concerning the sample sintered at 1300 °C is that for x = 1.0 the Pr_2CoO_4 phase is not observed. At high (1350 °C) sintering temperature, a densification occurs through the liquid phase and the temperature where the eutectic appears depends strongly on the system's composition.

The Figures 2a, 2b and 2c show micrographs of the samples sintered at 1300 °C. In all cases dense ceramics (>95% of theoretical density) were obtained with presence of inter- and intragranular pores, in small amounts. For x = 1.0 the intragranular pores were completely eliminated, indicating that Pr_6O_{11} helps densification. Pr_6O_{11} strongly influences the grain size, which gets its maximum average value of 30 μm for x = 0.5 (see Table 1). Figures 2d, 2e and 2f show micrographs of the samples sintered at 1350 °C. The presence of a larger amount of precipitates in the grain boundary is

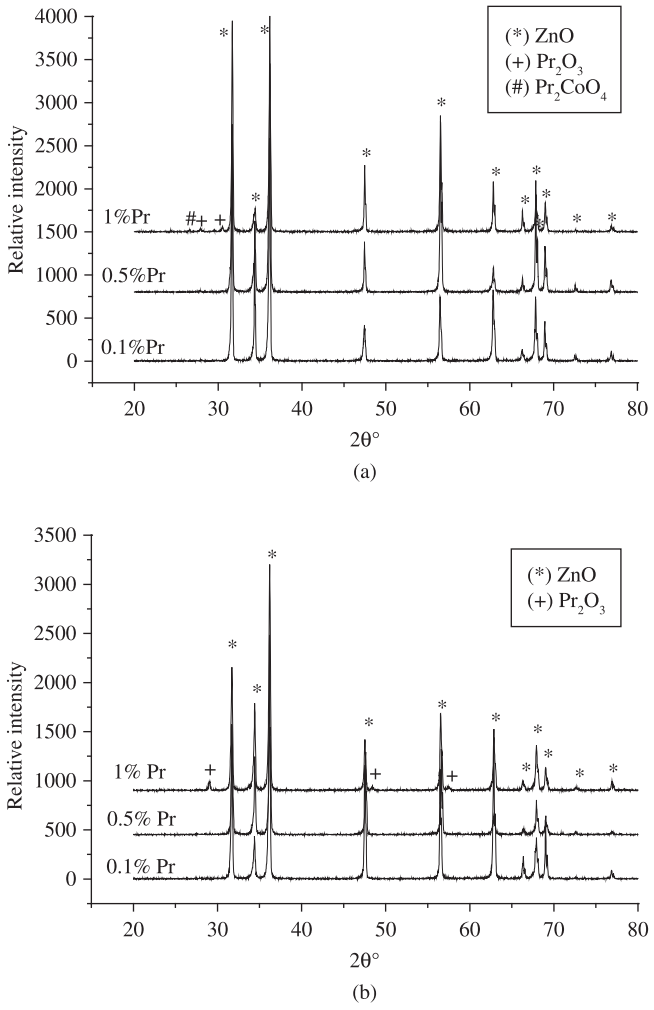

Figure 1. XRD patterns of ZPC with a different content of Pr_6O_{11} additive, indicating phases of samples sintered at a) 1300 °C and b) 1350 °C.

an obvious indication for the liquid phase of all compositions, at the temperature interval between 1300 and 1350 °C. Micrographs show that the average grain size reaches a maximum when x = 0.5. The increase of the average grain size by addition of a small amount of dopant (x = 0.5) may be caused by some lattice defects, similar to that related to the La doped $BaTiO_3$[17], which is reported elsewhere. Further addition of Pr_6O_{11} above 0.5 mol% causes the suppression of grain growth (except for the sample with x = 1.0 mol% and sintered at high temperature). Such suppression has been also reported for 2 mol% rare-earth (Sm, Eu, Y and Er) doped ZnO. The reason for this suppression has been attributed to the pinning effect during the movement of grain boundaries[18-19]. In the light of variations of intergranular material, the liquid phase formation temperature is expected to occur between 1300 and 1350 °C depending on the system's composition. The crystals generation for the sample with x = 1 and sintered at 1350 °C suggests that the liquid phase has the lowest temperature formation in this case. EDS analysis (not shown) determined that the precipitated phase is Pr-rich.

Figure 3a and 3b show the nonohmic behavior (*E* vs. *J*) of ZPC varistors sintered at 1300 and 1350 °C, respectively. More detailed concerning the *E* vs. *J* characteristic parameters, including the breakdown electric field (*Eb*), leakage current (I_L), nonlinear coefficient (α), are summarized in Table I. The amount of 0.5 mol% Pr_6O_{11} is

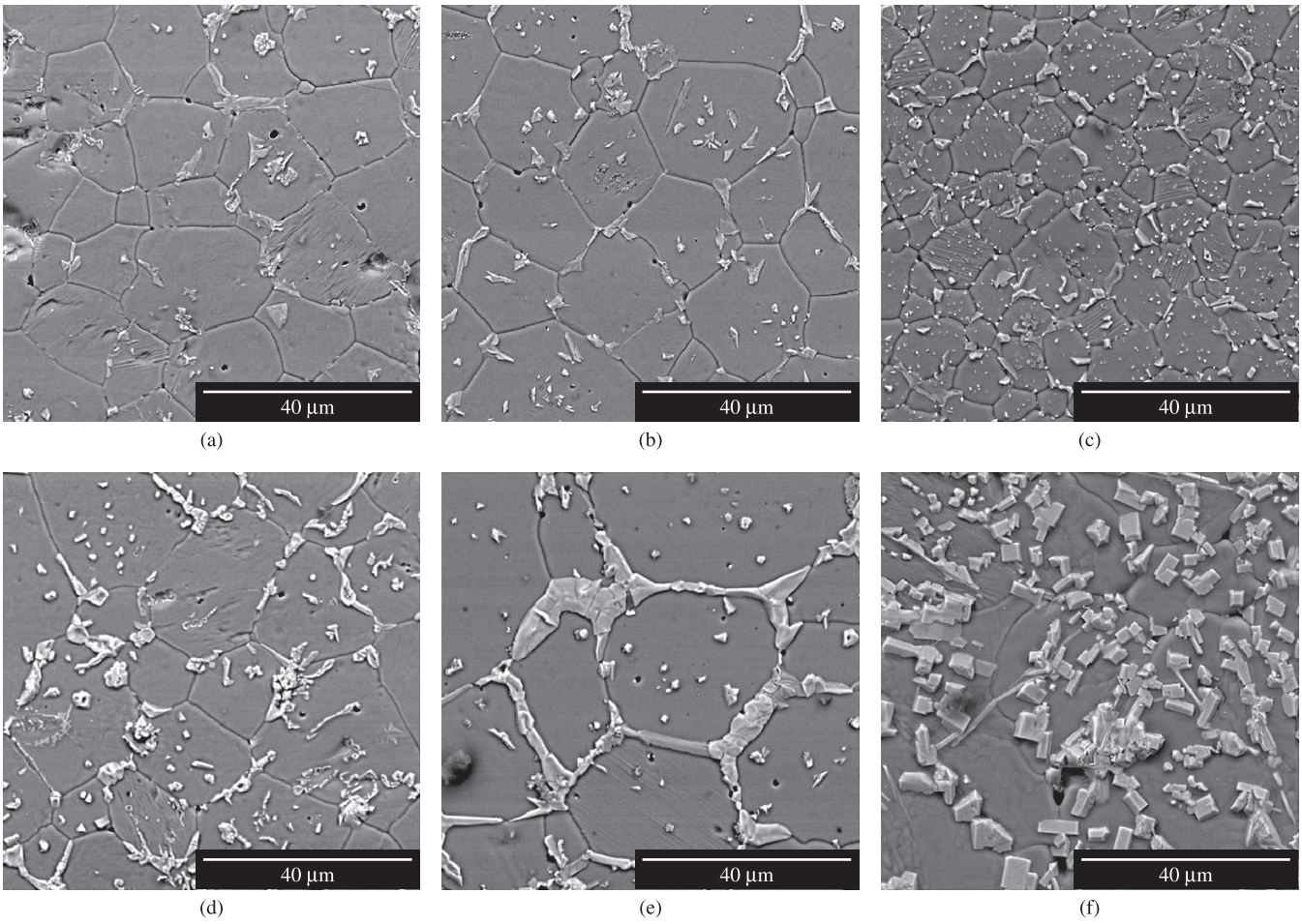

Figure 2. SEM micrographs of ZPC ceramics with different content of Pr_6O_{11} additive: a) and d) 0.1% Pr_6O_{11}, b) and e) 0.5% Pr_6O_{11}, c) and f) 1.0% Pr_6O_{11}. The samples of micrographs showed in Figures a), b), c) have been sintered at 1300 °C and d), e), f) at 1350 °C.

Table 1. The current-voltage (*I-V*) and capacitance-voltage (*C-V*) characteristic parameters of ZPC varistors with different content of Pr_6O_{11} additive sintered at 1300 and 1350 °C. The nonlinear coefficient (α) has been calculated for range values between 1-10 mA/cm^2 and leakage current (I_L) calculated at 20% of the breakdown electrical field.

Samples*	E_b (V/cm) ± 100	I_L (µA) ± 1	α ± 10	d (µm) ± 1	N_d (m^{-3}) ($\times 10^{24}$) ± 0.02	N_{IS} (m^{-2}) ($\times 10^{16}$) ± 0.01	ϕ_B (eV) ± 0.01	ω (nm) ± 0.02
0.1 (1300)	1050	174	9.0	22	1.17	2.08	0.454	10.3
0.1 (1350)	308	217	6.5	26	1.01	2.30	0.483	9.86
0.5 (1300)	201	210	3.8	30	-	-	-	-
0.5 (1350)	40	613	1.7	33	-	-	-	-
1.0 (1300)	1584	235	8.2	11	0.68	1.34	0.286	10.0
1.0 (1350)	425	287	5.5	35	0.57	2.04	0.674	8.5

*The first number indicates Pr_6O_{11} amount, the second number that this between parentheses indicates the sintered temperature.

not appropriate for varistors properties. This can be associated with the presence of a small number of effective barriers in the grain boundaries, besides the grain growth, generating few barriers among electrodes. The nonohmic properties have a significant increase for x = 1.0, as the highest value of the breakdown electric field since this dopant level inhibits grain growth, as shown by SEM.

It can be observed from Table I, that the nonohmic behavior of 0.1 mol% Pr_6O_{11} doped system sintered at 1300 °C is superior when compared with the sample with the same composition sintered at 1350 °C. This indicates, that the liquid phase is important for homogenizing dopants, but the electric properties of this phase is as well an important aspect. For instance, praseodymium has several oxidation states in the ZnO-based varistors, which can change dramatically the electrical behavior. The valence change is very sensitive to the applied process, as well as the Pr_6O_{11} amount. This aspect should be carefully evaluated. In ZnO.Bi_2O_3-based varistor systems, changes also occur in both phases, the amorphous and crystalline phase of Bi_2O_3 during the processing or its useful life[7, 20]. The varistors submitted to different stresses during use can modify its crystalline structure, which can cause the degradation process[7].

Figures 4a and 4b show Nyquist complex impedance diagrams for ZPC system with 0.1 and 1 mol% of Pr_6O_{11} and sintered at 1300 and 1350 °C respectively. The inset of the region shows high frequencies. Two semicircles are observed which indicate the presence of two time

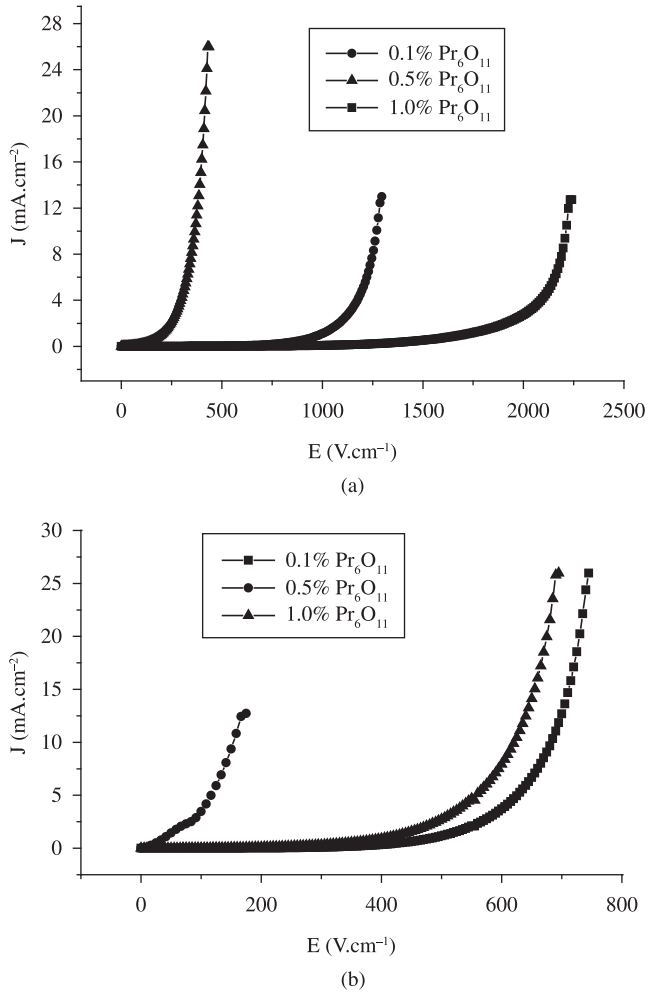

Figure 3. The current density-electric field (*J-E*) characteristics of ZPC varistors with different content of Pr_6O_{11} additive sintered at a) 1300 °C and b) 1350 °C.

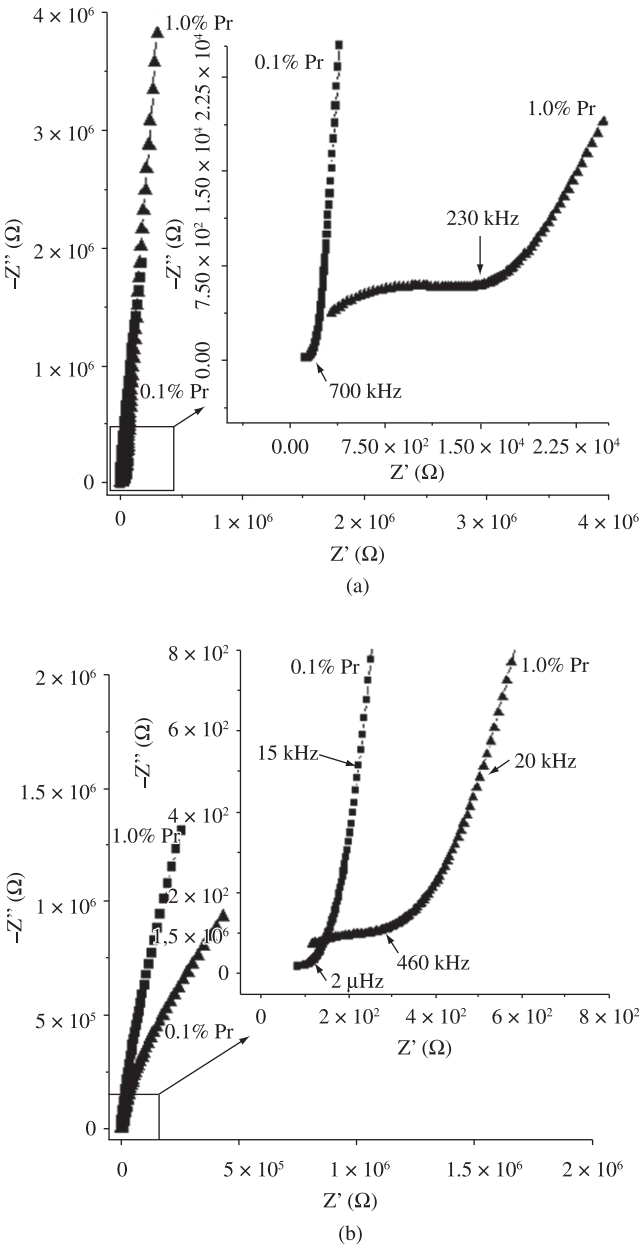

Figure 4. Nyquist diagram for ZPC system with 0.1 and 1.0 mol% of Pr_6O_{11} sintered at a) 1300 °C and b) 1350 °C.

constants in the systems. The samples sintered at 1350 °C showed more conductivity, this result occurs according to the leakage current values. The semicircles arcs in the complex moved with the center displaced below the real axis, because of the presence of distributed elements and relaxation process resulting from the trapped states.

Figures 5a and 5b show Nyquist complex capacitance behavior of the ZPC system with different content of Pr_6O_{11} and sintered at 1300 and 1350 °C, respectively. The capacitive complex diagrams for semiconductor polycrystalline devices are discussed in detail in reference[21] and reviewed in reference[22]. The samples sintered at 1350 °C possess a larger grain size, and therefore exhibit a higher capacitance than samples sintered at 1300 °C. The decrease of the amount of the grain boundary, resulting from a faster grain growth at higher liquid sintering temperature, makes a contribution to the increase of the capacitance of the ZnO varistors, a capacitance of grain boundary barrier-layer type, which depends on the grain size[23]. The accumulate defects in the grain boundary region can lead to this widening thus decreasing the grain boundary capacitance. The grain boundary capacitance is located in the transition region, while the electrical manifestation of the trapping states is evident in intermediate frequencies when the Mott-Schottky behavior is not satisfied. At low frequencies exists a conductive component (G/ω) related to the grain boundary resistance. A good linear relationship can be seen between the $(1/C - 1/2C_0)^2$ vs. *dc* voltage (except the samples with x = 0.5 and sintered at 1350 °C) indicating that the barriers formed at the grain boundaries of highly dense ZnO are of Schottky nature.

The corresponding Mott-Schottky plot is shown in Figures 6a and 6b. The observed frequency, depending on capacitance in conjunction with the information on grain size, reflects the averaged Mott-Schottky response. The ϕ_B, *Nd*, N_{IS} and ω values calculated from this averaged Mott-Schottky response is displayed in Table 1. It is observed in this table that increasing the temperature from 1300 to 1350 °C, *Nd* decrease due to oxidation of Zn donor defects[2]. *Nd* decrease is accompanied by an increase of interfacial states density N_{IS} and height barrier ϕ_B, as well as decrease of depletion layer ω. The values of barrier height ϕ_B are calculated based on the fact that all the grains are considered electroactive. The obtained values are small, indicating that not all the barriers are active. In ZnO-Bi_2O_3

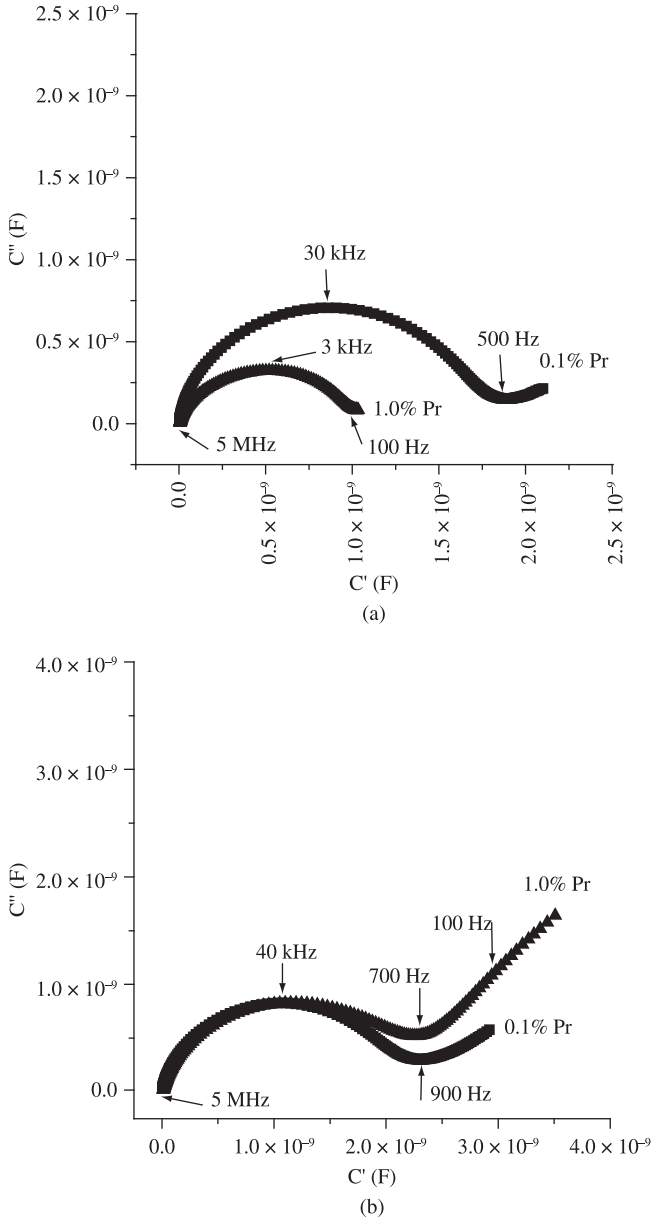

Figure 5. Complex capacitance behavior of the ZPC varistors systems with different content of Pr_6O_{11} additive biased at zero volts and sintered at: a) 1300 and b) 1350 °C.

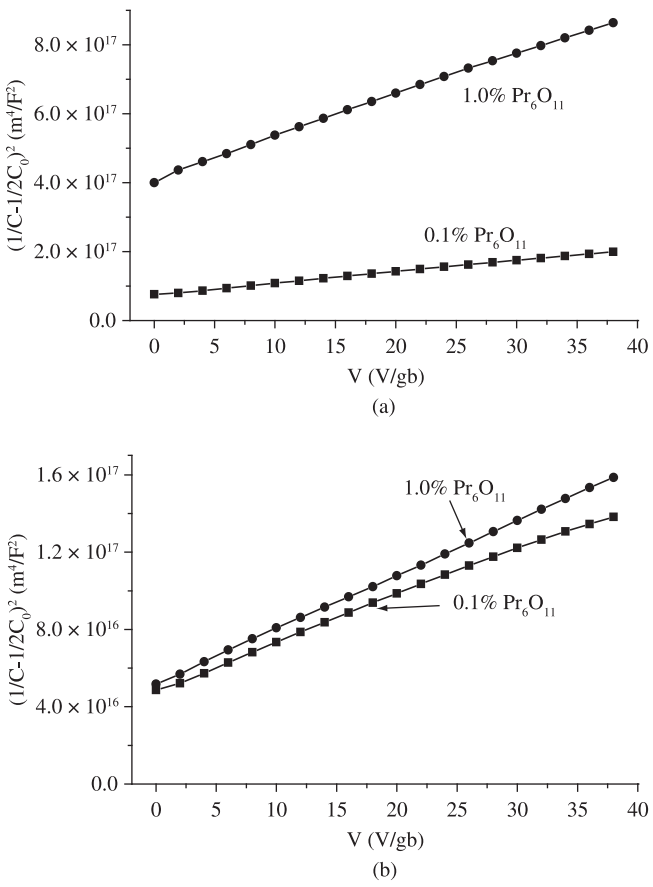

Figure 6. Mott-Schottky behavior without charge transport influence (true Mott-Schottky behavior) of ZPC varistors systems with different content of Pr_6O_{11} additive and sintered at: a) 1300 and b) 1350 °C.

based varistor the active potential barrier ranges from 15-35%[24-25] and SnO_2-based varistor 85% of the grain-to-grain junctions were active potential barriers[26-27]. For the sample with x = 0.5, the increase in the capacitance with bias voltage can be related to degradation in the nonohmic properties involving a distortion of the Schottky barriers at intergrains. A change in the donor concentration profile would directly affect the conductivity and capacity of the samples.

4. Conclusions

The nonohmic and microstructural properties of the ZPC systems are very sensitive to Pr_6O_{11} contents and the sintering temperature. The best behavior is obtained for the system with 0.1 mol% of Pr_6O_{11}, sintered at 1300 °C. However, samples doped with 0.5 mol% of Pr_6O_{11} showed to be very conductive (specifically the sintered sample at 1350 °C which does not follow a Mott-Schottky behavior), this aspect is related to a lower number of electrically active barriers. According to DRX, doping with 1.0 mol% Pr_6O_{11} generates secondary phases of Pr_2O_3 and the properties have been recovered, showing similar electric parameters like the samples doped with 0.1 mol% Pr_6O_{11}. SEM analyses showed that all compositions contain precipitates Pr-rich, which should be carefully studied, specifically regarding the oxidation state and their influence on the nonohmic properties. ZPC systems own a simpler microstructure than ZnO.Bi_2O_3 traditional varistors and a potential application for low-tension varistors. However new dopants should be used in order to increase the potential barrier and decrease the leakage current.

Acknowledgements

The authors gratefully acknowledge the financial support of the Brazilian agency FAPESP and the CYTED Program (Protect PI-VIII.13 PROALERTA).

References

1. Levinson LM and Pilipp HR. Zinc oxide varistor-a review. *American Ceramic Society Bulletin*. 1986; 65(4):639-646.
2. Lee YS, Liao JS and Tseng TY. Microstructure and crystal phases of praseodymium oxides in zinc oxide varistor ceramics. *Journal of the American Ceramic Society.* 1996; 79(9):2379-2384.

3. Alles AB and Burdick VL. The effect of liquid-phase sintering on the properties of Pr_6O_{11}-based ZnO varistors. *Journal of the Applied Physics*. 1991; 70(11):6883-6890.
4. Mukae K, Tsuda K and Nagasawa I. Nonohmic properties of ZnO-rare earth metal oxide-Co_3O_4 ceramics. *Japanese Journal of the Applied Physics*. 1977; 16(8):1361-1368.
5. Nahm CW and Park CH. Effect of Er_2O_3 addition on the microstructure, electrical properties, and stability of Pr_6O_{11}-based ZnO ceramic varistors. *Journal Materials Science*. 2001; 36(7):1671-1679.
6. Ramírez MA, Bueno PR, Ribeiro WC, Varela JA, Bonett DA, Villa JM et al. The failure analyses on ZnO varistors used in high tension devices. *Journal Materials Science.* 2005; 40(21):5591-5596.
7. Ramírez MA, Simões AZ, Márquez MA, Maniette Y, Cavalheiro AA, Longo E et al. Characterization of the ZnO-degraded varistors used in high-tension devices. *Materials Research Bulletin*. 2007; 42(6):1159-1168.
8. Ramírez MA**,** Bassi W**,** Bueno PR, Longo E and Varela JA. Comparative degradation of ZnO- and SnO_2-based polycrystalline non-ohmic devices by current pulse stress. *Journal of Physics D: Applied Physics*. 2008; 41(12):122002.
9. Ramírez MA**,** Cilense M, Bueno PR, Longo E and Varela JA. Comparison of non-Ohmic accelerate ageing of the ZnO- and SnO_2-based voltage dependent resistors. *Journal of Physics D: Applied Physcis*. 2009; 42(1):015503.
10. Lee YS and Tseng TY. Phase identification and electrical properties in ZnO-glass varistors. *Journal of the American Ceramic Society*. 1992; 5(6):1636-1640.
11. Nahm CW and Park CH. Microstructure, electrical properties and degradation behavior of praseodymium oxides-based zinc oxide varistors doped with Y_2O_3. *Journal Materials Science*. 2000; 35(12):3037-3042.
12. Hang HH and Knowles KM. Microstructure and current-voltage characteristics of praseodymium-doped zinc oxide varistors containing MnO_2, Sb_2O_3 and Co_3O_4. *Journal Materials Science*. 2002; 37(6):1143-1154.
13. Mukae K. Zinc oxide varistors with praseodymium oxide. *American Ceramic Society Bulletin*. 1987; 66(9):1329-1331.
14. Nahm CW. The electrical properties and dc degradation characteristics of Dy_2O_3 doped Pr_6O_{11}-based ZnO varistors. *Journal of the European Ceramic Society*. 2001; 21(4):545-553.
15. Wurst JC and Nelson JA. Linear intercept technique for measuring grain size in two-phase polycrystalline ceramics. *Journal of the American Ceramic Society*. 1972; 55(2):109-110.
16. Mukae M, Tsuda K and Nagasawa I. Capacitance vs voltage characteristics of ZnO varistor. *Journal of the Applied Physics*. 1979; 50(6):4475-4476.
17. Drofenik M. Oxygen partial pressure and grain growth in donor-doped $BaTiO_3$. *Journal of the American Ceramic Society*. 1987; 70(5):311-314.
18. Jorgensen PJ and Andersen PC. Modification of sintering kinetics by solute segregation in Al_2O_3. *Journal of the American Ceramic Society*. 1965; 48(4):207-209.
19. Kingery WD, Bowen HK and Uhlmann DR. *Introduction to Ceramics*. 2nd ed. New York: Wiley; 1976. p. 171-448.
20. Ramírez MA, Simões AZ, Bueno PR, Márquez MA, Orlandi MO and Varela JA. Importance of oxygen atmosphere to recover the ZnO-based varistors properties. *Journal of Materials Science*. 2006; 41(19):6221-6227.
21. Bueno PR, Varela JA and Longo E. Admittance and dielectric spectroscopy of polycrystalline semiconductors. *Journal of the European Ceramic Society*. 2007, 27(13-15): 4313-4320.
22. Bueno PR, Varela JA and Longo E. SnO_2, ZnO and related polycrystalline compound semiconductors: An overview on the voltage dependent resistance (non-ohmic) feature. *Journal of the European Ceramic Society*. 2008, 28(3):505-529.
23. Burn I and Neirman S. Dielectric properties of donor-doped polycrystalline $SrTiO_3$. *Journal Materials Science*. 1982; 17(12):3510-3524.
24. Clarke DR. The microstructural location of the intergranular metal-oxide phase in a zinc oxide varistor. *Journal of the Applied Physics*. 1978; 49(4):2407-2411.
25. Tao M, Ai B and Dorlanne O. Loubiere A. Different "single grain junctions" within a ZnO varistor. *Journal of the Applied Physics*. 1987; 61(4):1562-1567.
26. Vasconcelos JS, Vasconcelos NSLS, Orlandi MO, Bueno PR, Varela JA, Longo E et al. Electrostatic force microscopy as a tool to estimate the number of active potential barriers in dense non-ohmic polycrystalline SnO_2-based devices. *Applied Physics Letters*. 2006; 89(15):152102.
27. Ramírez MA, Bassi W, Parra R, Bueno PR, Longo E and Varela J.A. Comparative electrical behavior at low and high current of SnO_2 and ZnO based varistors. *Journal of the American Ceramic Society*. 2008; 91(7):2402-2404.